EARTHQUAKE ENGINEERING AND STRUCTURAL DYNAMICS
Earthquake Engng. Struct. Dyn. **27**, 811–824 (1998)

VIBRATION CONTROL OF CABLE-STAYED BRIDGES—PART 1: MODELING ISSUES

ARMIN G. SCHEMMANN[1,*] AND H. ALLISON SMITH[2]

[1] *Novellus Systems Inc., 3970 N. First St., San Jose, CA 95134, U.S.A.*
[2] *Department of Civil Engineering, Stanford University, Stanford, CA 94305-4020, U.S.A.*

SUMMARY

The objective of the research presented here is to increase the understanding of how the complexities associated with modeling cable-stayed bridges, such as non-linear behaviour and the participation of highly coupled, high-order vibration modes in the overall dynamic response, affect the overall effectiveness of active control schemes. The 316-degree-of-freedom analytical model studied here is based on the Jindo Bridge located in South Korea. Computational considerations associated with control analyses require the size of the model to be significantly reduced, without loss of the important vibration characteristics and complexities. Three separate reduced-order modelling techniques for creating effective control models are studied here: the IRS method, the internal balancing method, and a modal reduction method. These methods are studied and compared on their ability to capture the complex dynamic response of cable-stayed bridges subjected to multiple-support excitation and their ability to create viable and computationally sound state-space models for control analyses. Results show that the modal reduction technique, because of the ability to select only those modes causing the largest force and displacement response, is most effective for control applications.

KEY WORDS: cable-stayed bridge; active control; reduced-order model; seismic response; multiple-support excitation

INTRODUCTION

In structural engineering, the mitigation of damage induced by large environmental loads is of paramount interest. Specifically, in seismic regions, earthquakes can pose a threat to human lives and the infrastructure. In recent years, the idea of applying active control as a means of hazard reduction has grown increasingly popular. In essence, through the application of actuators and sensors, active control can reduce structural forces and vibrations such that desirable performance characteristics are achieved. Although significant strides have been made in recent years towards the development and application of active control schemes for vibration control of civil structures in seismic zones, its application to large lifeline structures, such as cable-stayed bridges, under earthquake loading has not been addressed extensively.

This paper is one of two parts describing research with the objective of obtaining an understanding of how the complexities associated with cable-stayed bridges affect the overall effectiveness of active control schemes. The analytical bridge model used here is based on the Jindo Bridge located in South Korea. The full-order finite element bridge model used in this study has 316 degrees-of-freedom. Non-linearities are considered by performing a non-linear static analysis (prior to a linear dynamic analysis), in which the stiffness matrix associated with the dead load deformed shape is obtained. To achieve maximum effectiveness and practicality, control algorithms require the size of the model to be reduced significantly, without loss of the important

* Correspondence to: Armin G. Schemmann, 2722 Byron Street, Palo Alto, CA 94306, U.S.A. E-mail: armin@gofannon.stanford.edu
Contract/grant sponsor: National Sceince Foundation; Contract/grant number: BCS-9317722-001

CCC 0098–8847/98/080811–14$17·50

Received 5 October 1997

vibration characteristics and complexities. Three reduced-order modelling techniques are presented and studied here: the Improved Reduced System (IRS) method, the internal balancing method, and a modal reduction method. These methods are studied for their ability to effectively capture the complex behaviour of cable-stayed bridges subjected to multiple-support excitation while allowing for substantial reduction of computational intensity when used as state-space control models.

This paper discusses the modelling issues associated with representing the dynamic behaviour of cable-stayed bridges. Three reduced-order modelling techniques are presented together with a summary of their effectiveness when applied as control models. An introduction of active control issues and a description of the proposed actuator layout is provided. This paper concludes with a summary of the important issues to be considered when developing models for control analysis of cable-stayed bridges. Part 2 of this research presents and describes the control analyses performed using the model developed here.

PREVIOUS WORK

While research in the area of active control has advanced considerably in the past decades, only limited research has been directed towards cable-stayed bridges. Using a continuous system model to represent a bridge with four cable-stays, Yang *et al.*[1,2] performed some of the earliest work in this area, when they studied the application of active control to cable-stayed bridges under the excitation of strong wind gusts. Warnitchai *et al.*[3] experimentally and analytically studied control of cable-stayed bridges subject to a vertical sinusoidal force utilizing a simple cable-supported cantilever as a model. Hutton[4] used active control to control vertical deflections of a cable-stayed guideway under a moving constant load. Using a simply supported, lumped mass beam supported by two cables, Volz *et al.*[5] employed a decentralized active controller to reduce the bridge's vertical deck deflections and Magaña *et al.*[6] examined robust non-linear active control to attenuate displacements under adverse conditions. Achkire *et al.*[7] experimentally and analytically examined active vibration control of cables and cable systems using a single active tendon. To a certain degree, active control technology for cable-stayed bridges overlaps with the active control technology developed for large space structures. Both areas consider large mathematical models which exhibit a large number of vibration modes within the frequency band of the external disturbance/excitation. The paper by Hyland *et al.*[8] presents a wealth of information on the state of the art of active control technology for large space structures.

MODELING CABLE-STAYED BRIDGES

The presence of cable elements and a complex structural geometry cause geometrical non-linearities in the behaviour of cable-stayed bridges. Specifically, these non-linearities are due to: (1) the axial force deformation relationship of the inclined cables caused by the deadweight induced sag; (2) the axial force–bending moment interaction of the towers and longitudinal girders (i.e. beam–column interaction); and (3) the geometry change due to large deformations. A non-linear static analysis is performed to obtain the stiffness matrix associated with the dead-load deformed shape and is followed by a linear dynamic analysis[9–11]. Material non-linearities, which are typically avoided for such large structures, are not included. Other complexities associated with the cable-stayed bridge include: (1) multiple support excitation, caused by the exposure of the bridge towers to the spatially random seismic excitation; and (2) the participation of coupled, high-order, three-dimensional vibration modes in the overall dynamic response. To model the non-linear axial force deformation relationship of the bridge cables, the catenary-shaped cables are replaced by single straight cords with equivalent moduli of elasticity. The beam–column interaction exhibited by the support towers and deck are represented through the use of stability functions in developing the stiffness matrix for the beam elements. Finally, the geometric non-linearity caused by large (static) deformations is considered by applying the dead load in a stepwise fashion and continuously updating the geometry of the structure. A combined Newton–Raphson and Euler (stepwise) procedure is used as a non-linear solution strategy. The finite element

computer code has been modified in accordance with the work presented by Fleming *et al.*[9] and Nazmy *et al.*[10]

The three-dimensional Finite Element Model (FEM) used in this study represents a 1–150 experimental scale model built to Garevski and Severn's[12] blueprints, and measures 3·23 m in length. The FEM has 147 nodes, 106 elements and 504 rigidly linked Degrees Of Freedom (DOF) yielding a 316 DOF model. A single central spine with lumped masses attached is used to represent the deck. Space frame elements are used to model the deck and the towers. Rigid links are used to represent the offset between the cables and the spine. In addition, to inducing coupling of the torsional and transverse modes of the deck, rotary inertia of the masses is included at the appropriate degrees of freedom. The girder is supported vertically and laterally by the towers; however, the base of the tower is considered sufficiently rigid, such that the fixed tower base and the girder supported at the tower are subject to the same translational ground motion. Hence, the girder is modeled to be vertically and laterally constrained rather than being linked to the tower.

In this study, two approaches are used to implement multiple-support excitation. In the first approach the spatial variation is considered by using recovered earthquake records of synchronized, closely spaced arrays. This method was successfully used in Nazmy *et al.*,[13] in which the 1979 Imperial Valley earthquake records were considered. In the second and more simplistic approach, a single earthquake record is used, and a time delay in the support motions is added to account for the change in phase of the input motions. This method, which only accounts for the traveling wave effect, is further simplified by only considering the case in which the supports move 180° out of phase relative to the adjacent supports. This second method, which illustrates one of the worst-case scenarios of the travelling wave effects, is used in the majority of this study to illustrate the effects of multiple-support excitation. Both methods induce phase differences in the support motions causing non-inertial or kinematic (pseudostatic) motion unique to multiple-support excitation. Pseudo-static forces are induced by the differential static ground displacements between the individual supports and are not present in uniform support excitation.

DYNAMIC RESPONSE OF BRIDGE MODEL

Table I lists the first 20 undamped natural frequencies of the finite element model. For illustrative purposes, Figure 1 displays the first-order torsional mode (7), fifth-order vertical mode (8), fourth-order lateral deck mode (20) and the first longitudinal tower mode (18). It is observed that the model has mode shapes which span all three dimensions and that many modes are coupled; hence, a three-dimensional model is clearly required and ground motion should have components in all three orthogonal directions. Modal coupling is less dominant in the lower modes; however, the coupling and the complexity of the individual modes increase

Table I. Undamped natural frequencies of FEM and scaled prototype

Mode no.	FEM model freq. (Hz)	Scaled prototype freq. (Hz)	Mode no.	FEM model freq. (Hz)	Scaled prototype freq. (Hz)
1	4·441	0·360	11	26·18	2·137
2	6·539	0·534	12	26·38	2·154
3	9·141	0·746	13	28·35	2·315
4	12·42	1·014	14	29·04	2·371
5	14·16	1·156	15	29·13	2·378
6	18·46	1·507	16	32·49	2·653
7	21·69	1·772	17	35·88	2·929
8	22·71	1·855	18	35·89	2·930
9	24·97	2·039	19	37·92	3·096
10	25·63	2·093	20	39·92	3·259

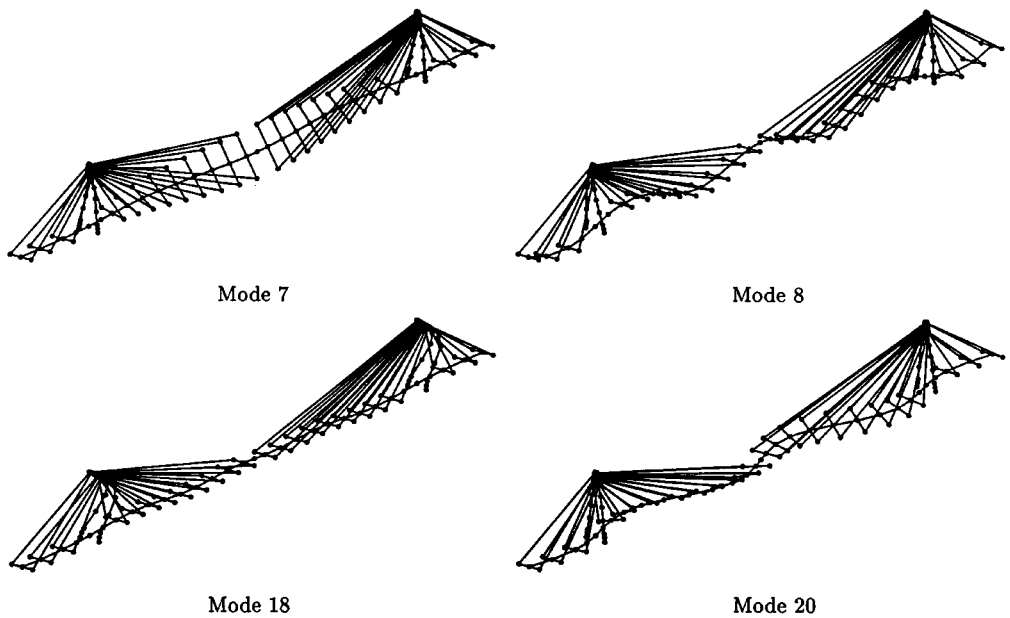

Figure 1. FEM mode shapes 7, 8, 18, 20

with increasing mode number. For instance, the first two lateral deck modes are virtually uncoupled from any other mode, while almost all higher lateral deck modes also have some torsional component.

Next, time-history analyses are performed to obtain the modes that participate most dominantly in the structure's force response. Generally, sensors and actuators should be positioned such that all major participating modes (i.e. those which should be controlled) are observable and controllable. Locations close to or on a nodal point of an important mode should be avoided. For cable-stayed bridges, the extent to which modes participate depends on two parameters: the direction of earthquake excitation and the type of ground motion excitation, which can be classified as either uniform or multiple-support excitation. Uniform-support excitation typically excites symmetric modes whereas multiple-support excitation often excites antisymmetric modes.

The model is studied using two earthquake records: one ground motion is from the 1994 Northridge earthquake, while multiple ground motions (to model multiple-support excitation) are from the 1979 Imperial Valley earthquake. The horizontal component of the 1994 Northridge earthquake (Los Angeles–Baldwin Hills reading) with a peak ground acceleration (PGA) of $0{\cdot}25g$ is used to supply the ground motion record for the majority of this study. This record is chosen because its accelerations act over a wide range of frequencies, even though this ground motion is not necessarily reflective of the local site conditions of the Jindo Bridge. Array 4, 5, 6 and 7, representing closely spaced records of the 1979 Imperial Valley earthquake (PGA between $0{\cdot}16g$ and $1{\cdot}7g$) are used for the case when multiple-support excitation is modelled using earthquake records of synchronized, closely spaced arrays. The acceleration response spectra of a horizontal component of the Northridge and Imperial Valley earthquake (Array 5) are illustrated in Figure 2.

The time-history analyses are performed using modal superposition. To examine the extent to which modes participate in the response of the bridge deck, modal superposition analyses are performed using individual modes to form the modal mass and stiffness matrices. Detailed results pertaining to time history force response of the towers can be found in Schemmann and Smith.[14] Time-history analyses for the cases of uniform and multiple-support excitation are performed using the principle of modal superposition in which

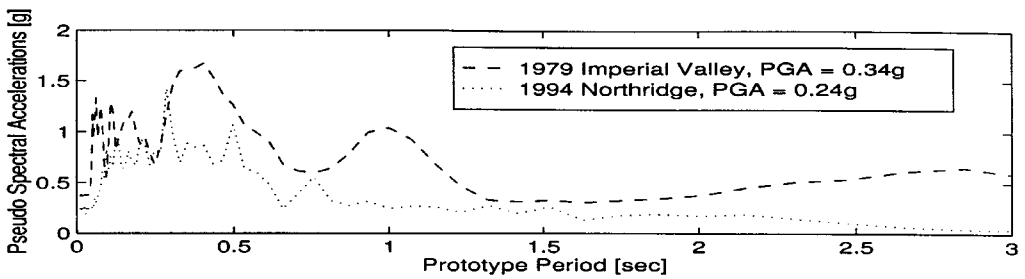

Figure 2. Pseudo-spectral accelerations for horizontal component of Array 5 of Imperial Valley earthquake and Los Angeles-Baldwin Hills record of Northridge earthquake

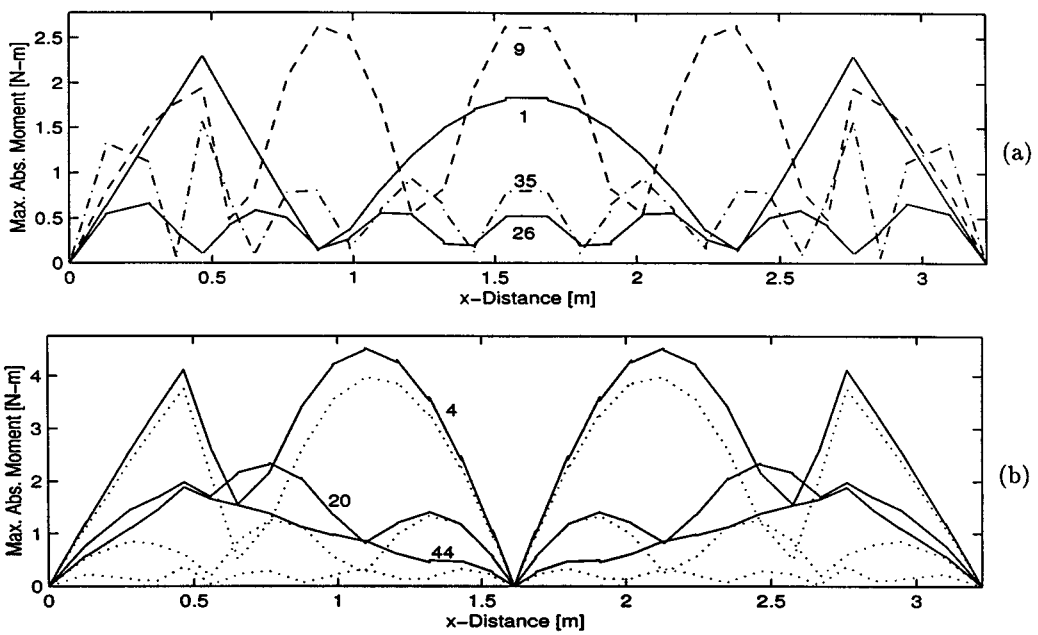

Figure 3. Lateral deck bending moment envelope using: (a) modes 1, 9, 26, 35 subject to lateral uniform excitation and; (b) modes 4, 20, 44 subject to lateral multiple-support excitation

the first 100 modes are applied individually. Modes above 100 are not considered, since modes in the range of 50 to 100 do not participate significantly in the structure's force response, and the participation of even higher modes is not expected.

Figure 3 shows the peak lateral deck bending moments as a function of the bridge span coordinate (x) for modes 1, 9, 26, and 35 under lateral uniform-support excitation and for modes 4, 20 and 44 under multiple-support excitation. The dotted lines which appear in the plots for multiple-support excitation cases show the moments due to vibrational motion, whereas the solid lines show the total moment due to both vibrational and pseudo-static motion. Since pseudo-static motion is unique to multiple-support excitation, the dashed line overlaps the solid line for the uniform support excitation cases. The dashed lines, which appear in the plots for uniform-support excitation cases have no special indication and are solely used to

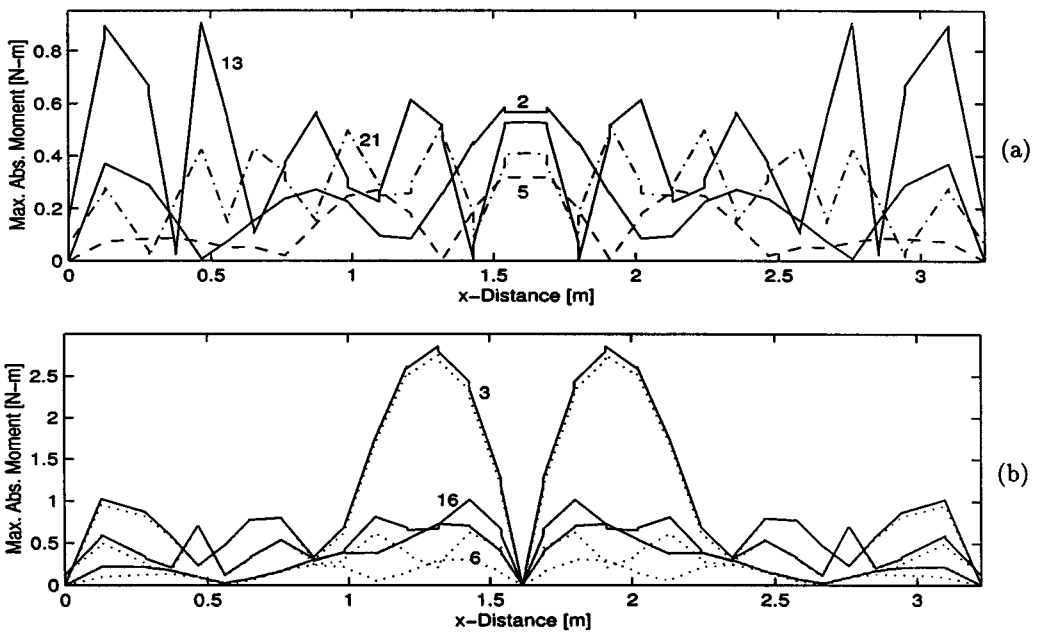

Figure 4. Vertical deck bending moment envelope using: (a) modes 2, 5, 13, 21 subject to vertical uniform excitation and; (b) modes 3, 6, 16 subject to vertical multiple-support excitation

differentiate the various lines. For the case of uniform-support excitation, the largest moments are induced by modes 1 and 9, which represent the first and the third lateral deck modes. The higher modes 26 and 35 also produce significant moments and should not be ignored in a full modal analysis. For the case of multiple-support excitation, mode 4 dominates the response, while mode 44 contributes little to the force response. Similarly, Figure 4 shows the peak vertical deck bending moments for modes 2, 5, 13 and 21 under vertical uniform-support excitation and for modes 3, 6 and 16 under multiple-support excitation. For the former case, all modes contribute significantly to the force response. For the case of multiple-support excitation, mode 2 representing the first vertical deck mode dominates the response. Figure 5 shows that modes 3, 6, 10, and 18 need to be considered to capture the full force response of the deck due to longitudinal uniform-support excitation. Mode 18, which is predominantly a tower mode, produces the largest moments for this case due to coupling action between the tower and the deck. Under longitudinal multiple-support excitation, modes 5 and, especially, mode 2 dominate the response.

Analyses are also carried out where a number of modes are applied as a set to form the modal matrices. The results of these analyses identify the most damaging modes and indicate the modes to be included in modal analyses using multiple modes. Results of these analyses are expressed in terms of maximum absolute bending moments obtained over the duration of the ground motion. Figure 6 shows the peak lateral deck bending moments as a function of the bridge span coordinate (x), in which modes are applied in the sets 1-1, 1-9, 1-26, 1-35 (under lateral uniform excitation) and 1-4 and 1-20 (under multiple-support excitation), for the modal superposition analysis. Figure 7 shows the peak vertical deck bending moments using modes 1-2, 1-30 (under vertical uniform excitation) and 1-3 and 1-16 (under multiple-support excitation). Figure 8 shows the peak vertical deck bending moments using modes 1-3, 1-10, 1-28 (under longitudinal uniform excitation) and 1-2 and 1-8 (under multiple-support excitation). Figures 6–8 are obtained considering the Northridge earthquake and the simplified case of multiple-support excitation. Modal analyses using larger sets of modes

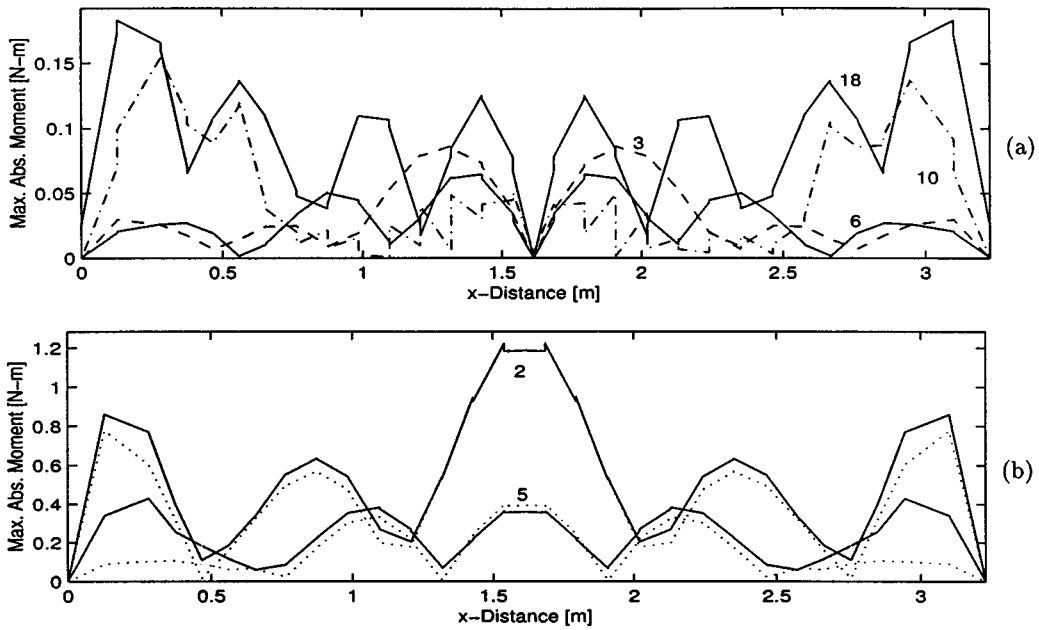

Figure 5. Vertical deck bending moment envelope using: (a) modes 3, 6, 10, 18 subject to longitudinal uniform excitation and; (b) modes 2, 5 subject to longitudinal multiple-support excitation

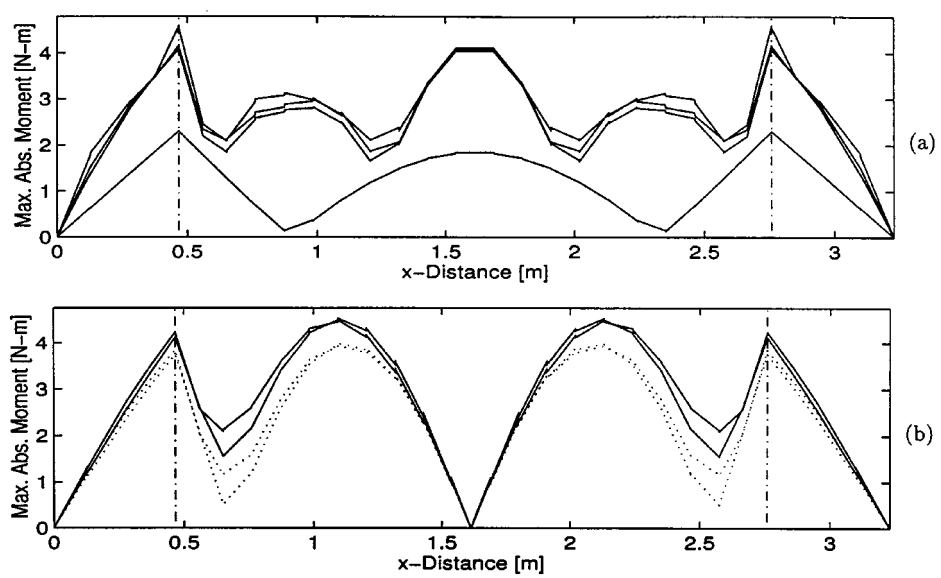

Figure 6. Lateral deck bending moment envelope using: (a) modes 1, 1–9, 1–26, 1–35 subject to lateral uniform excitation and; (b) modes 1–4, 1–20 subject to lateral multiple-support excitation

were also performed; however, the additional modes had little influence on the results. Of the multiple lines presented in Figures 6–8, the lower lines represent the cases in which only a few modes are used in the sets, while the upper lines typically represent the cases in which more modes are included.

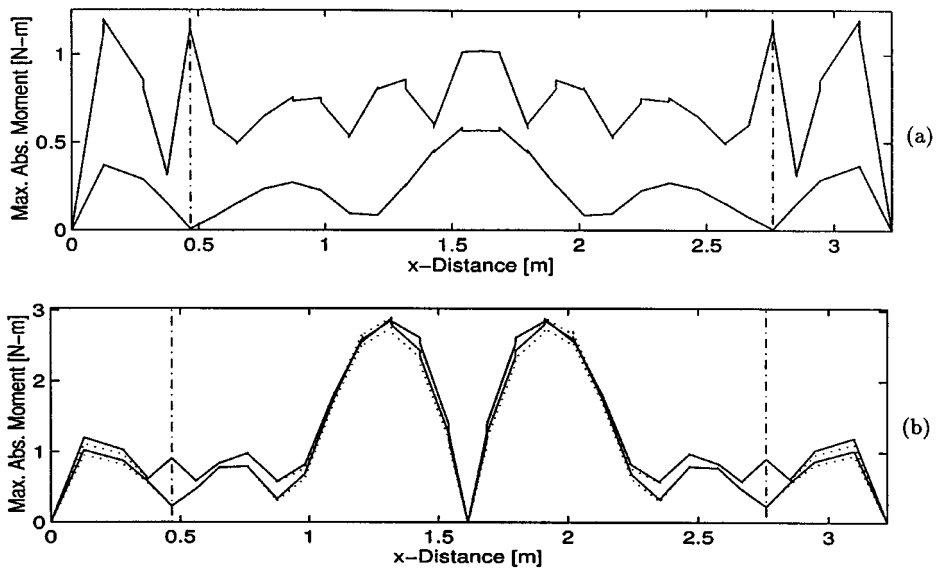

Figure 7. Vertical deck bending moment envelope using: (a) modes 1–2, 1–30 subject to vertical uniform excitation and; (b) modes 1–3, 1–16 subject to vertical multiple-support excitation

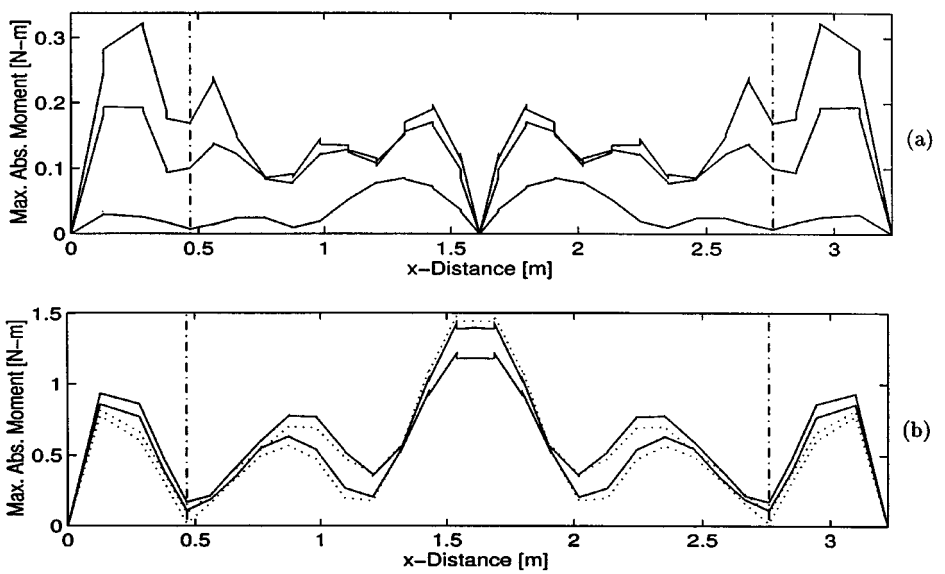

Figure 8. Vertical deck bending moment envelope using: (a) modes 1–3, 1–10, 1–28 subject to longitudinal uniform excitation and; (b) modes 1–2, 1–8 subject to longitudinal multiple-support excitation

Numerous conclusions can be drawn from the time-history analyses. The time-history analyses confirm the importance of multiple-support excitation. Compared to uniform-support excitation, bending moments are increased significantly at numerous bridge deck locations, in part due to the pseudo-static displacements. Moreover, under multiple-support excitation an entirely different set of modes is excited resulting in a different response of the bridge. The time-history analyses also display the locations at which maximum

internal forces can be expected. This information is helpful in effectively locating actuators and sensors. Furthermore, the modes which need to be controlled are highlighted. The drawback of these time-history analyses is that, in this case, they are only valid for this particular earthquake record. Different earthquakes have different frequency content and, thus, may excite other modes. Thus, time-history analyses should be performed using a larger set of ground motions to obtain more general results. Results of the time-history analyses using the Imperial Valley earthquake can be found in Schemmann and Smith.[14] These results indicate that the Imperial Valley earthquake excites fewer modes (especially higher order ones) than the Northridge earthquake.

Quite often for building structures, the modes which cause the largest displacements also generate the largest forces, so that displacement control will also automatically control the internal forces. However, this is not necessarily the case here. Since higher-order modes, which do not significantly participate in the displacement response, participate significantly in the force response, the control algorithm will have to insure that the internal forces and not just displacements are reduced.

REDUCED-ORDER MODELING FOR CONTROL

Since most control algorithms work best for structures with few degrees of freedom, the current finite element model with 316 degrees of freedom is too large in size. Hence, to achieve maximum effectiveness and mathematical viability for control algorithms, it is necessary to obtain a reduced-order model. A multitude of model reduction techniques of varying complexity are available in literature. Reduction techniques examined in this study included O'Callahan's improved reduced system (IRS) reduction,[15] a model reduction using the internal balancing method as introduced by Moore,[16] and a reduced modal modelling technique. While other reduction methods were considered, they were generally dismissed because they did not provide sufficient accuracy based on previously published results, or they were considered mathematically inefficient.

IRS method

The IRS method is based on the Guyan reduction technique, which in essence uses static condensation to remove undesired secondary degrees of freedom from both the mass and stiffness matrix. However, the IRS method improves on the Guyan reduction by including mass effects in the transformation matrix. The first step in the IRS method involves forming a static transformation matrix based on the Guyan reduction. Next, to estimate mass effects, a dynamic transformation matrix is formed using the static transformation matrix from the preceding step. The final transformation matrix, which is derived from the static and dynamic transformation matrices, is applied to mass, stiffness and damping matrices. The derivation of this method and its equations can be found in the paper by O'Callahan.[15]

Since vertical and lateral vibrational deck modes are generally decoupled, an attempt is made to obtain the smallest possible reduced-order model by creating two reduced-order model—one to predominantly capture the lateral vibrational characteristics of the bridge and another to capture the vertical behaviour. Once both models are obtained, control algorithms are to be applied to the two separate systems. As a result, two sets of control gains are obtained, which are to be combined and applied to the full-order model. The validity of this superposition of control gains depends on the amount of coupling between the lateral and vertical mode shapes. The superposition will not be valid if the modes are strongly coupled, since vibrations and control forces in the lateral (or vertical) direction would spill over to the vertical (or lateral) direction, effectively altering the vertical (or lateral) system's characteristics. This change in system dynamics would most likely render the vertical (or lateral) system suboptimal or even unstable. Inadequacy of the models based on this issue would indicate the necessity of a single reduced-order model capturing both vertical and lateral dynamics.[14]

The models capturing the lateral and vertical vibrational characteristics could be reduced by a maximum of 240 DOFs each, yielding two 86 DOF models. Reductions beyond 240 DOFs either did not warrant the

Table II. Condition numbers of stiffness, mass and system matrices

Condition numbers	Full-order model	Reduced-order model	
		Lateral	Vertical
Stiffness matrix	1·91e + 07	1·66e + 14	6·01e + 15
Mass matrix	2·67e + 05	4·19e + 13	7·85e + 16

trade-off between the smaller model sizes and loss of accuracy. Generally, the reduced-order models (ROM) captured most of the natural frequencies and mode shapes corresponding to deck motion with good accuracy. However, the dynamics of the tower, which are only scarcely represented in terms of unreduced (primary) DOFs, are captured subadequately. Furthermore, the ROMs introduced some undesirable spurious modes that are not present in the full-order model (although these modes do not seem to participate significantly in the bridge's force response).

Nevertheless, the problem with these reduced-order models does not necessarily lie in the loss of accuracy in dynamics they incur, but that an 86 DOF model (172-order state-space model) is still very large for control purposes. Moreover, an IRS model reduction to this degree introduces severe ill-conditioning in the reduced stiffness and mass matrix. The normal effect of severe ill-conditioning on the solutions of matrix equalities is to produce erratic answers, thus rendering the stiffness and mass matrix inappropriate for any additional reductions or computations. Table II shows the condition number for the reduced stiffness and mass matrices. For this instance, the condition numbers imply that any computations involving these matrices cannot be relied upon to have any accuracy unless significantly more than 15 or 16 figures are carried. Computations in this study are only carried out to 16 significant figures considerably limiting the use of these matrices for any further calculations.

In summary, the 86 DOF vertical and lateral reduced order models offer only subadequate representations of the full order model. Too much ill-conditioning is introduced and yet the model still remains too large for control purposes. Hence, the IRS method proves to be an inappropriate choice of model reduction for this type of structure. Additional information and a more detailed discussion of these analyses and results can be found in Schemmann and Smith.[14]

Reduction by internal balancing method

The internal balancing method was first introduced by Moore[16] and further refined and extended in other studies.[17, 18] In contrast to the previous method, this technique is directly applied to the linear control system

$$\dot{\mathbf{x}}(t) = \mathbf{A}\mathbf{x}(t) + \mathbf{B}_u\mathbf{u}(t) + \mathbf{B}_w\mathbf{w}(t) \tag{1}$$

$$\mathbf{y}(t) = \mathbf{C}\mathbf{x}(t) + \mathbf{D}\mathbf{u}(t) + \mathbf{J}\mathbf{w}(t) \tag{2}$$

where $\mathbf{x}(t)$ is the state vector, $\mathbf{u}(t)$ is the vector of control inputs, $\mathbf{y}(t)$ is the vector of sensor measurements, $\mathbf{w}(t)$ is the vector of disturbance inputs and $\mathbf{A}$, $\mathbf{B}_u$, $\mathbf{B}_w$, $\mathbf{C}$, $\mathbf{D}$ and $\mathbf{J}$ are system matrices of the appropriate dimensions. The objective of this method is to reduce those states which are the least controllable and observable. In essence, controllability and observability indicate to which degree a state's response can be affected and measured by the given actuator and sensor configuration.

To implement this strategy, the controllability and observability Gramians, which measure the degree of controllability and observability, respectively, are required. For an asymptotically stable system the controllability and observability Gramian, $\mathbf{W}_c$ and $\mathbf{W}_o$, can be obtained from the algebraic Lyapunov

equations

$$\mathbf{A}\mathbf{W}_c + \mathbf{W}_c\mathbf{A}^T + \mathbf{B}\mathbf{B}^T = 0 \tag{3}$$

$$\mathbf{A}^T\mathbf{W}_o + \mathbf{W}_o\mathbf{A} + \mathbf{C}^T\mathbf{C} = 0 \tag{4}$$

Next, transformations are applied to Equations (1), (2) and the Gramians under a change of state coordinates $\mathbf{x}_r(t) = \mathbf{T}\mathbf{x}(t)$ where $\mathbf{T}$ is non-singular, to obtain the set of transformed matrices $\tilde{\mathbf{A}} = \mathbf{T}^{-1}\mathbf{A}\mathbf{T}$, $\tilde{\mathbf{B}} = \mathbf{T}^{-1}\mathbf{B}$, $\tilde{\mathbf{C}} = \mathbf{C}\mathbf{T}$, $\tilde{\mathbf{D}} = \mathbf{D}$, $\tilde{\mathbf{J}} = \mathbf{J}$, $\tilde{\mathbf{W}}_c = \mathbf{T}^{-1}\mathbf{W}_c\mathbf{T}^{-T}$ and $\tilde{\mathbf{W}}_o = \mathbf{T}^{-T}\mathbf{W}_o\mathbf{T}$ with respect to $\tilde{\mathbf{x}}$ co-ordinates. The matrix $\mathbf{T}$ is formed such that both $\tilde{\mathbf{W}}_c$ and $\tilde{\mathbf{W}}_o$ are diagonal and in this case equal to each other, i.e. balanced. The balancing transformation matrices, $\mathbf{T}$ and $\mathbf{T}^{-1}$, are given by

$$\mathbf{T} = \mathbf{L}_c\mathbf{V}\Sigma^{-1/2},\ \mathbf{T}^{-1} = \Sigma^{-1/2}\mathbf{U}^T\mathbf{L}_o^T \tag{5}$$

where $\mathbf{U}$, Σ and $\mathbf{V}$ are obtained from the singular value decomposition $\mathbf{L}_o^T\mathbf{L}_c = \mathbf{U}\Sigma\mathbf{V}^T$, in which $\mathbf{L}_c$ and $\mathbf{L}_o$ denote the lower triangular Cholesky factors of the Gramians $\mathbf{W}_c$ and $\mathbf{W}_o$. A detailed derivation and discussion of the transformation matrix is given by Laub *et al.*[17] It can be shown that

$$\tilde{\mathbf{W}}_c = \tilde{\mathbf{W}}_o = \Sigma = \mathrm{diag}(\sigma_1, \sigma_2, \ldots, \sigma_k, \ldots, \sigma_{2n}) \tag{6}$$

where σ_i denotes the ith term (singular value) of the singular value matrix, Σ. The singular values, σ_i's, which are arranged in descending order, indicate the degree of controllability and observability of the corresponding transformed state $(x_r)_i$. For some index $k+1$ the value σ_{k+1} will be much smaller than the preceeding value σ_k, indicating low controllability and observability. Hence the states $(x_r)_{k+1}$ to $(x_r)_{2n}$ are discarded during the reduction, while the states $(x_r)_1$ to $(x_r)_k$ are retained. Correspondingly, a reduced system is obtained by retaining the matrix partition of dimension $k \times k$ of $\tilde{\mathbf{A}}$, the first k rows of $\tilde{\mathbf{B}}_r$, and the first k columns of $\tilde{\mathbf{C}}_r$.

Laub *et al.*[17] mention that the computation of balanced realizations for the case of large, sparse models remains a challenging open problem. This problem was alleviated when the model is put into modal form in which a reduced set of modes, for instance one including the first 100 modes, is considered. Since the reduction is directly correlated to controllability and observability, the reduction were very sensitive to actuator and sensor layout. Hence, the most damaging modes were not necessarily captured, but instead the dynamics which could be observed and controlled best.

For this study, four actuators and sensors are placed on the centre span acting in both lateral and vertical directions. Reduced-order models were created using 25, 50, and 100 balanced states; however, none of them produced acceptable results. While the 25 and 50 state models could not adequately capture the model's dominant natural frequencies, the 100 state model was already too large for control purposes. All three ROMs had difficulties capturing higher-order modes and vertical deck dynamics, especially for the case of multiple-support excitation. The quality of the models were based on a comparison of singular value plots in which vertical and lateral frequency responses were measured at various deck locations subject to uniform and multiple-support excitation. Since a modal model is required for the balanced reduction, it may be more efficient to create a reduced-order model simply using a smaller modal model without applying any additional reductions. A more detailed discussion of these findings can be found in Schemmann and Smith.[14]

Reduction by modal superposition

Here, important modes are identified and used as a set to form the modal transformation matrix, Φ, leading to the reduced system equations:

$$\mathbf{A}_r = \begin{bmatrix} \mathbf{0} & \mathbf{I} \\ -\mathbf{\Lambda} & -\mathrm{diag}(\Sigma_1^n 2\omega_i\xi_i) \end{bmatrix} \quad \mathbf{B}_r = \begin{bmatrix} \mathbf{0} \\ \mathbf{\Phi}^T\mathbf{B} \end{bmatrix} \quad \mathbf{C}_r = \mathbf{C}\begin{bmatrix} \mathbf{\Phi} & \mathbf{0} \\ \mathbf{0} & \mathbf{\Phi} \end{bmatrix} \tag{7}$$

in which eigenvectors are mass-orthonormalized, modal damping is used to create the damping matrix, n represents number of modes used for the superposition, $\mathbf{\Lambda} = \mathrm{diag}(\omega_1^2, \omega_2^2, \ldots, \omega_n^2)$, ω_i and ξ_i are the ith

natural frequency and modal damping value, respectively. Although, typically the lower 1 to n modes are used in consecutive order in a modal superposition, not all modes within this range need to be considered. Modes which participate significantly in the overall response of the structure must be included, while other modes can be left out. This method has to its advantage that a very accurate reduced-order model can be obtained without sacrificing the conditioning of the mass and stiffness matrices. Furthermore, the analyst has good control over the ROM's dynamics by selectively including or excluding modes from the transformation matrix. Moreover, a model sufficiently small for control purposes can be formed. The modes which are represented in the ROM are accurate without introducing any spurious dynamics as is the case for the IRS reduction. Finally, as compared to the balanced reduction method, the transformed states can be easily visualized, giving the analyst better intuitive understanding of the model and any expected results. In controlling these states, control effort is applied directly to the individual modes.

Prior to selecting the modes used for the modal superposition, the participation of each mode in the force response must be known. This information can be obtained from the time-history analyses performed earlier (see Figures 3–8), which highlight the dominant modes. Enough modes are used when the solution has converged sufficiently, i.e. additional modes do not affect the solution. For this study, the set of modes consists of modes 1 to 6, 8 to 11, 13 to 21, 26 and 35 yielding a 42-order state-space model and representing the first six primarily lateral deck modes, the first primarily vertical deck modes, five tower modes and one coupled tower/deck mode. This set captures all the important modes participating in the bridge's force response when subjected to the Northridge and Imperial Valley earthquakes. The set does not include any torsional deck modes, since none of them are significantly excited by translational ground motion.

In summary, this method provides means of accurately reducing the model to a sufficiently small size for control purposes. Furthermore, the transformed states are in a visualizable format, giving the analyst intuition of the expected model behaviour. For all its advantages, this method is used to reduce the full-order model.

OVERVIEW OF ACTIVE CONTROL

Throughout this study, the Linear Quadratic Regulator (LQR) control theory is applied to the 42-order state-space model described above. This method is used because it is very effective and can be applied intuitively. Furthermore, when working in the modal space, control efforts can be directed to individually specified modes, giving the designer great flexibility. Control analyses using this method are performed in Part 2 of this research.

Two types of control schemes are used. First, control analyses are performed using full state feedback control, in which all states are assumed to be known at all times. Next, analyses are performed employing output feedback control, in which all states are extrapolated from a few measured states using a Kalman filter estimator. Since full state feedback control produces better results in terms of vibration control, it yields an upper bound on the performance of output feedback control. Although not as realistic as output feedback control, full state feedback control, which also requires less computational effort, is applied to the bridge to examine the (maximum) effectiveness of active control in attenuating the bridge's force time-history response. Later, output feedback control utilizing accelerating feedback is applied to examine the degradations in the performance of active control that can be anticipated when employing output feedback control. Various sensor locations are also examined to improve the performance of output feedback control.

In this study, the LQR control algorithm is evaluated, actuator and sensor locations are chosen, and simulations are performed to evaluate the effectiveness of active control. Hardware issues, such as actuator design, are considered beyond the scope of this study and, hence, are not addressed. For the majority of this research, actuators and sensors are assumed to be collocated. Configurations using 4, 6 and 8 actuators (and sensors) are considered, of which half act in each lateral and vertical directions. Generally, actuators are positioned such that all major participating modes are controllable to a high degree. For instance, in the case of lateral uniform and multiple-support excitation, it is desirable to primarily control modes 1, 4 and 9, which

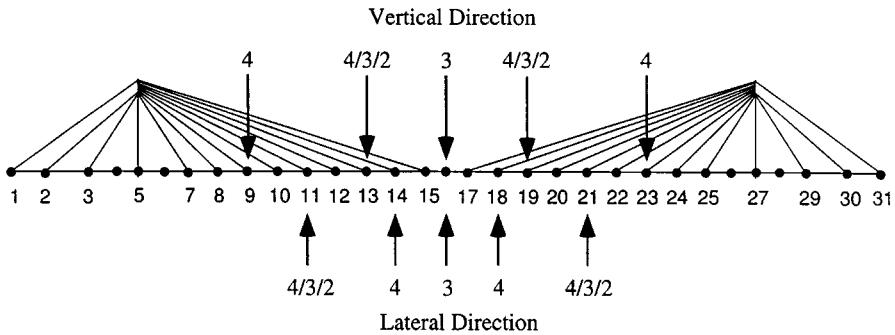

Figure 9. Actuator and sensor arrangement for lateral and vertical deck vibrations. Numbers (2, 3, and 4) indicate that the actuator is used for the cases when 2, 3 and 4 actuators are used

cause the largest bending moments in the deck (see Figures 6 and 3). Modes 20, 26 and 35, which are also important, but induce lower moments than modes 1, 4 and 9, should be controllable through at least one actuator. Therefore, desirable locations for actuators acting in the lateral direction include deck nodes 11, 14, 16, 18 and 21. Specifically, when considering the use of 4 actuators in the lateral direction, actuators are placed at deck nodes 11, 14, 18 and 21. For the case when 3 or 2 actuators are considered, actuators are located at nodes 11, 16 and 21, or nodes 11 and 21, respectively. Comparing the actuator locations to the maximum bending moment envelopes illustrated in Figure 6, it can be seen that, for modes 1, 4 and 9, at least one of the actuators is always close to or right on an apex of the bending moment envelopes for all actuator setups, rendering these modes highly controllable. Furthermore, modes 20, 26 and 35 are all controllable since, for any actuator configuration, at least one actuator is located away from a nodal point. The final actuator locations are illustrated in Figure 9.

Actuator locations for the vertical direction are obtained through a similar procedure. Here, Modes 2, 3 and 13 induce the largest deck bending moments under vertical and longitudinal support excitation (uniform and multiple) as can be seen in Figures 4 and 5. Thus, actuator configurations for vertical direction should focus on the controllability of these modes. The configurations should also render modes 5, 10, 16, 18 and 21 controllable, since their participation in the deck's force response cannot be neglected. Locations for actuators acting in the vertical direction include deck nodes 9, 13, 16, 19, and 23 (see Figure 9). For the case when 4, 3, or 2 actuators are considered, actuators are placed at deck nodes 9, 13, 19 and 23, deck nodes 13, 16 and 19, or deck nodes 13 and 19, respectively. Comparing these actuator locations to the maximum bending moment envelopes in Figures 4 and 5 shows that all the above-mentioned modes are controllable (especially modes 2, 3 and 13).

CONCLUSIONS

As shown in prior research on cable-stayed bridges, results here indicate that high-order modes participate in the structural response. Furthermore, multiple-support excitation can cause a significant increase in structural forces and, hence, should be included in the analysis. Of the three model reduction techniques studied, the modal reduction method proves to be most promising because of its ability to select only those modes which cause the largest force and displacement response. Using this method, the final reduced-order state-space model has 42 states, which capture the most damaging vibration behavior, and is computationally manageable for control analysis purposes. The IRS and balanced reduction methods yielded models which were too inaccurate and too large for control purposes and, in the case of the IRS method, introduced severe ill-conditioning in the mass and stiffness matrices, rendering the final state-space control model unusable.

ACKNOWLEDGEMENTS

The work presented herein was sponsored by the National Science Foundation (NSF) under Grant No. BCS-9317722-001. The financial support provided by this organization is gratefully acknowledged.

REFERENCES

1. J. N. Yang and F. Giannopoulos, 'Active control and stability of cable-stayed bridge', *ASCE J. Engng. Mech.* **105**, 677–694 (1979).
2. J. N. Yang and F. Giannopoulos, 'Active control of two-cable-stayed bridge', *ASCE J. Engng. Mech.* **105**, 795–810 (1979).
3. P. Warnitchai, Y. Fujino, B. M. Pacheco and R. Agret, 'An experimental study on active tendon control of cable-stayed bridges', *Earthquake Engng. Struct. Dyn.* **22**, 93–111 (1993).
4. D. V. Hutton, 'Dynamic analysis of active-control, cable-stayed guideway, *J. Struct. Engng.* **119**, 2403–2420 (1993).
5. P. Volz, M. E. Magana, A. G. Henried and T. H. Miller, 'A decentralized active controller for cable-stayed bridges', In *1st World Conf. on Structural Control*, Vol. 3, FA1-13, August 1994.
6. M. E. Magana, A. G. Henried and D. Scheer, 'Robust active control of cable-stayed bridge subject to earthquake ground motion', *Anal. Comput.* (1994) 317–326.
7. Y. Achkire and A. Preumont, 'Active tendon control of cable-stayed bridges', *Earthquake Engng. Struct. Dyn.* **25**, 585–597 (1996).
8. D. C. Hyland, J. L. Junkins and R. W. Longman, 'Active control technology for large space structures', *J. Guidance, Control Dyn.* **16**, 801–821 (1993).
9. J. F. Fleming and E.A. Egeseli, 'Dynamic behavior of a cable-stayed bridge', *Earthquake Engng. Struct. Dyn.* **8**, 1–16 (1980).
10. A. S. Nazmy *et al.*, 'Non-linear earthquake-response of long-span cable-stayed bridges. applications, *Eaerhquake Engng. Struct. Dyn.* **19**, 63–76 (1990).
11. A. S. Nazmy *et al.*, 'Non-linear earthquake-response of long-span cable-stayed bridges theory', *Earthquake Engng. Struct. Dyn.* **19**, 45–62 (1990).
12. M. A. Garevski and R. T. Severn, 'Damping and response measurement on a small-scale model of a cable-stayed bridge', *Earthquake Struct. Dyn.* **22**, 13–29 (1993).
13. A. S. Nazmy and A. M. Abdel-Ghaffar, 'Static and dynamic analysis of cable-stayed bridges subject to uniform and multiple-support excitations', *Technical Report 87-SM-1*, Princeton University, January 1987.
14. A. G. Schemmann and H. A. Smith, 'Modeling, and active control of cable-stayed bridges subject to multiple-support seismic excitation, *John A. Blume Earthquake Engineering Center Report No. 123*, Stanford University, Stanford, CA 94305, June 1997.
15. J. C. O'Callahan, 'A procedure for an improved reduced system (irs) model', in *7th Int. Modal Analysis Conf.*, 1989.
16. B. C. Moore, 'Principal component analysis in linear systems: controllability, observability and model reduction', *IEEE Trans. Automat. Control* **AC-26**, 17–32 (1981).
17. A. J. Laub, M. T. Heath, C. C. Paige and R. C. Ward, 'Computation of system balancing transformations and other applications of simultaneous diagonalization algorithms', *IEEE Trans. Automat. Control* **AC-32**, 17–32 (1987).
18. K. H. Yae and D. J. Inman, 'Model reduction in a subset of the original states', *J. Sound Vib.* **155**, 165–176 (1992).

